JOURNAL OF GEOPHYSICAL RESEARCH, VOL. 93, NO. C6, PAGES 6761-6773, JUNE 15, 1988

Entrainment and Homogenization of a Passive Tracer in a Numerical Model Gyre

ROBERT S. PICKART[1]

Woods Hole Oceanographic Institution, Woods Hole, Massachusetts

The mechanism by which tracer is entrained into a spatially decaying gyre from an external source is examined, as well as the homogenization which subsequently occurs. A simple advective-diffusive numerical model is used whose streamlines consist of an elongated gyre situated beside a distinct boundary current, which inputs tracer into the domain. This is meant to represent the deep cyclonic recirculation of the Gulf Stream and adjacent deep western boundary current. A shear flow analysis shows that two parameters dictate the manner in which tracer penetrates across streamlines of the gyre: a peclet number and a parameter which measures the strength of the cross-stream shear. The large values of these parameters cause a plume of tracer to spiral inward toward the center of the gyre. At steady state the tracer which has accumulated in the gyre becomes homogenized. The size of this uniform area is related to the extent to which the spiral penetrated the gyre and decreases with increasing diffusivity, as several examples illustrate.

1. INTRODUCTION

It is characteristic of closed streamline flow that properties in the interior become homogenized. This was shown explicitly by *Rhines and Young* [1982*a*], as applied to potential vorticity Q, provided the mixing due to eddies is weak. (Homogenization has been known to occur in the presence of strong mixing as well; see, for instance, Cox [1985].) The homogenization of Q is crucially tied to the structure of planetary scale circulation, as outlined by *Rhines and Young* [1982*b*] in their theory of wind-driven circulation. Regions of weak Q gradients are found persistently in eddy-resolving numerical models and have also been observed in data from the north Atlantic [*McDowell et al.*, 1982].

The main stream function and potential vorticity for the deep layer of a basin-wide quasi-geostrophic numerical model are shown in Figure 1 [from Holland and Rhines, 1980]. The area of uniform Q coincides with the region of most intense flow, thus showing the significance of the lateral extent of homogenization. In addition, the level of the homogenized plateau is related to the strength of the circulation. *Cessi et al.* [1987] examined the relationship between lateral extent and magnitude of homogenization and associated gyre circulation, and presented a way of calculating these quantities for the simplified case of a barotropic flow.

The smoothing of properties within closed streamlines reveals itself in another context as well: that of passive tracers. The simplified nature of passive tracers suggests that homogenization be examined in this framework, with the hope that insights revealed may be applied to the more complicated case of a dynamically active quantity. *Musgrave* [1985] conducted a numerical study of homogenization in a subtropical gyre, modeling the subduction of tracer from the sea surface. He examined both the aforementioned characteristics as a function of peclet number (which measures the relative strength of eddy mixing versus large-scale advection). The steady state distribution from one of the model simulations appears in Figure 2.

The direct ventilation mechanism that Musgrave modeled is not present in the deep ocean, whose density surfaces do not outcrop. Recently however, *Hogg et al.* [1986] discussed a case in which the properties of a deep recirculating flow are replenished in a straightforward manner. They outlined how the cyclonic recirculation of the deep Gulf Stream should pass close enough to the deep western boundary current (DWBC), west of the Grand Banks, to entrain relatively young, anomalous water diffusing from the DWBC. To investigate this process, they invoked a simple advective-diffusive numerical model; the streamlines of the model and situation which it proposes to represent are shown in Figure 3. The deep northern recirculation of the Gulf Stream has been studied extensively in recent years and is believed to transport roughly 20 sverdrups, deeper than 4000 m, between the Grand Banks and the New England seamounts. The reader is referred to *Hogg* [1983], *Hogg and Stommel* [1985], and *Hogg et al.* [1986] for both observational and theoretical discussions.

The advective-diffusive model of *Hogg et al.* [1986] was used to interpret hydrographic data collected in the region. The model circulation is highly idealized, and numerous potentially important aspects are omitted for simplicity, including multiple water mass sources. In addition, to parameterize the effect of eddies using a constant diffusivity represents an extreme simplification. There is evidence that the diffusivity in the western north Atlantic is a function of both lateral position and depth (J. Price, personal communication, 1986). The effects of different features such as these need to be examined in future investigations.

The results of the numerical model can also be reviewed independently, without direct comparison to the western north Atlantic, to study ideas pertaining to homogenization, which is the focus of this study. The flow field and boundary conditions of the model make this a particularly interesting case to investigate. In contrast to *Musgrave*'s [1985] model gyre, which is strongest at the outer edge, the gyre of Figure 3 decays at the edge, causing significant differences in entrainment of tracer by the gyre. In addition, the boundary conditions here are open (except for a small region of input)

[1]Now at Graduate School of Oceanography, University of Rhode Island, Narragansett.

Paper number 8C0121.
0148-0227/008C-0121$05.00

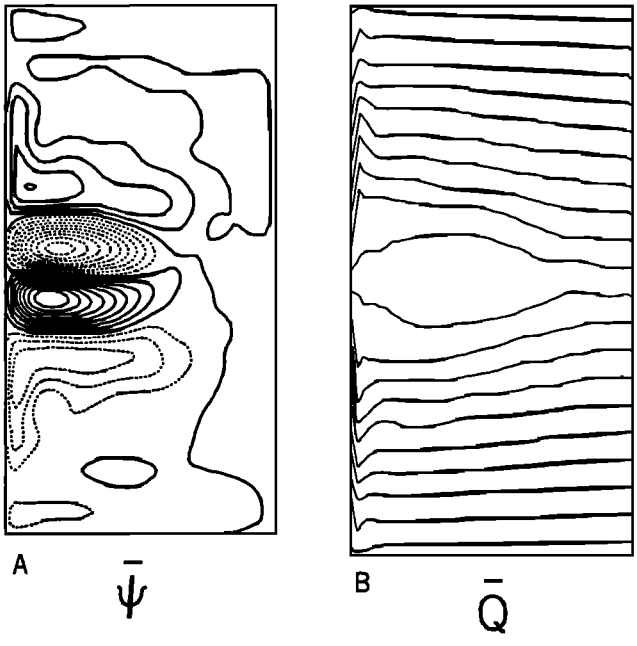

Fig. 1. Mean distribution (*a*) stream function and (*b*) potential vorticity, for the deep layer of a wind-driven eddy-resolving numerical model [from *Holland and Rhines*, 1980].

which allows the gyre itself to naturally determine the area which becomes homogenized. Thus it is not straightforward to predict the lateral extent of homogenization as a function of the model parameters. Similarly, it is not obvious what the final level of tracer will be in the gyre.

As part of their analysis, *Cessi et al.* [1987] derived a formula for diagnostically calculating the level of homogenization at steady state. This relation must hold in the present case, but it cannot tell us beforehand what the level will be, as there is limited boundary influence directly adjacent to the gyre. In the formulation used by *Cessi et al.* [1987] the strength of the mixing due to eddies is parameterized by the boundary conditions. In *Musgrave*'s [1985] simulation the gyre has a solid boundary. Such dependence of homogenization on boundary forcing is not present in this model.

The present study addresses the entrainment of tracer and how this is intimately tied to the occurrence of homogenization at steady state. Only the lateral extent of homogenization is considered, for any examination of the gyre level must include both the boundary current and gyre of Figure 3. Instead, we isolate the gyre circulation so as to keep the analysis more general.

First, the model is described and the manner of entrainment is isolated in the context of a simpler unidirectional flow. It is shown that the penetration of tracer across streamlines (which occurs as a plume extending from the boundary) can be characterized according to two parameters, which depend on the strength of the flow and the strength of its cross-stream shear, respectively. Results from this analysis are then applied to the full gyre circulation to explain an asymmetry in the plume of tracer as it penetrates the gyre interior.

Finally, the homogenization which occurs at steady state is described. The relationship between the size of the homogenized region and the plume of incoming tracer is examined, as well as the effect of varying the diffusivity.

2. The Advective-Diffusive Model

The evolution in time and space of a passive tracer is described by the advective-diffusive equation, considered here in its two-dimensional form

$$\theta_t + \mathbf{u}\cdot\nabla\theta = \nabla\cdot\kappa\nabla\theta \tag{1}$$

where $\theta(x,y)$ is the tracer concentration, κ is the eddy diffusivity (constant), $\mathbf{u}(x,y)$ is the horizontal velocity vector, and $\nabla = \mathbf{i}(\partial/\partial x) + \mathbf{j}(\partial/\partial y)$.

The flow field of Figure 3 is sufficiently complex that the solution for θ is obtained by a numerical integration. Specifically, (1) is finite-differenced forward in time, with upstream differencing for the advection and centered differencing for the diffusion. To counteract the implicit diffusion which accompanies upstream advection, at each time step a corrective measure was implemented, following the procedure of *Smolarkiewicz* [1983]. The test which Smolarkiewicz used on an isolated distribution of tracer was successfully applied here to check the scheme.

The model boundary conditions consist of three types. At the upstream edge of the southward flowing boundary current the concentration of tracer is specified as a gaussian distribution. At the downstream edge, tracer is allowed to advect out of the domain (at which location alongstream diffusion is omitted, which is a reasonable approximation in light of the strong current). Everywhere else along the boundary, velocities are negligibly small and thus were set identically equal to zero. In these regions an open boundary condition is employed, which allows tracer to diffuse out of the domain as if there were no boundary present. The method is based on an interior extrapolation at each time step and is described in the appendix.

Initially, there is no tracer within the domain. The diffusivity is set equal to $\kappa = 10^6$ cm^2/s (the circulation is steady). As time progresses, tracer is advected downstream and fills the boundary current, while slowly diffusing offshore. A plume develops as the eastward flow of the gyre pulls tracer away from the boundary. The plume then wraps around the gyre as tracer begins accumulating within it (Figure 4). Spin up continues in this manner until at steady state a homogenized region forms in the center portion of the gyre.

3. Entrainment

Close inspection of Figure 4 shows that as the plume of tracer winds around the gyre, it migrates across streamlines toward the gyre center. The reason for this spiral is that the

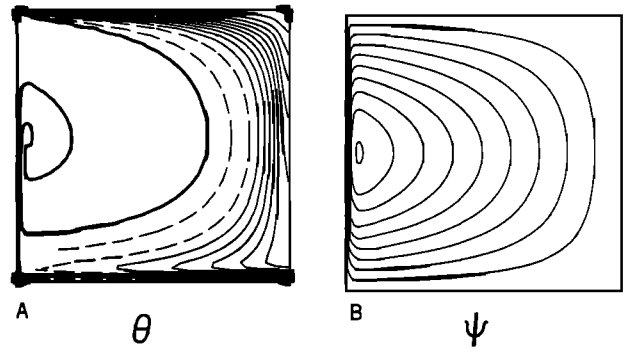

Fig. 2. (*a*) Isolines of a passive tracer θ at steady state for the circulation shown in (*b*), for the case of a large Peclet number [from *Musgrave*, 1985].

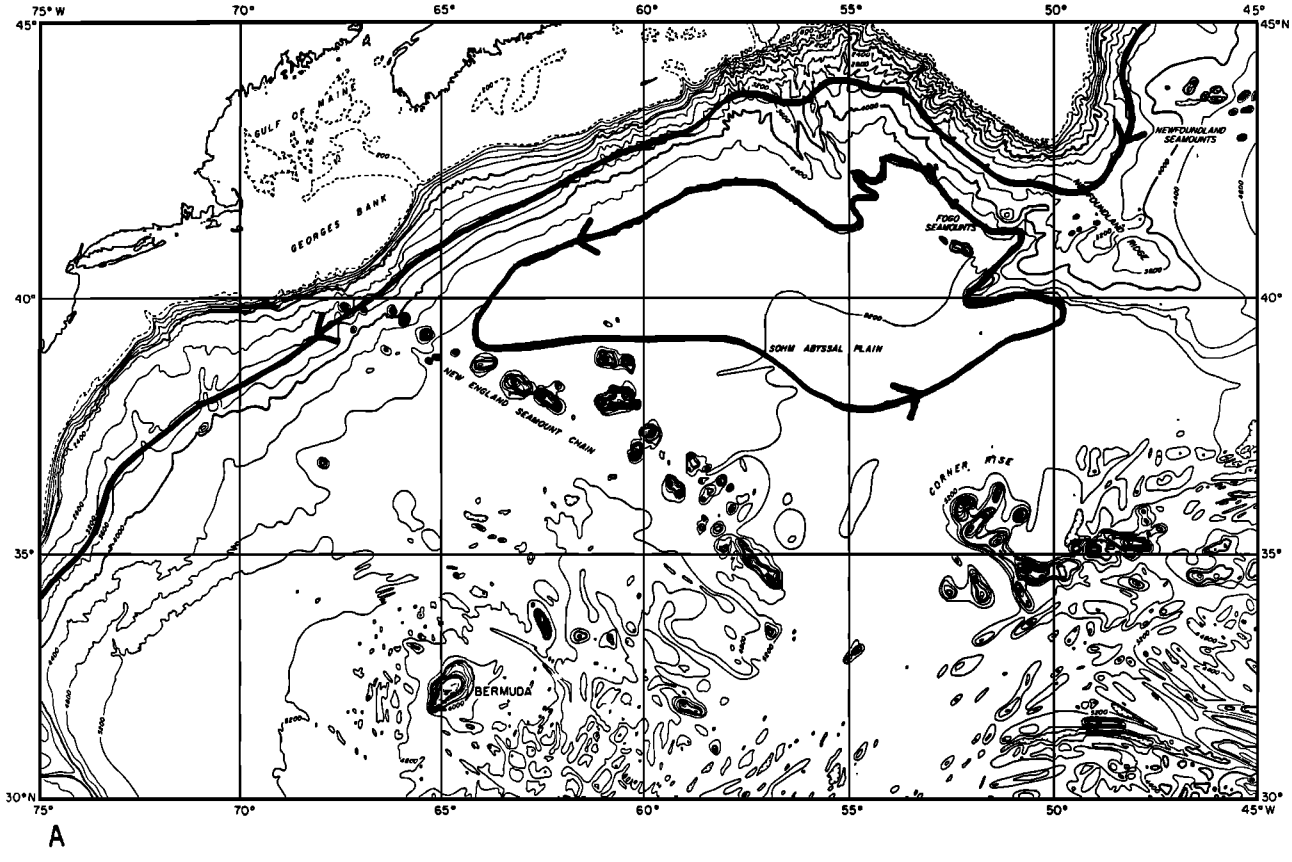

Fig. 3. (*a*) Schematic representation of the deep cyclonic Gulf Stream recirculation and DWBC. The gyre streamline is a deep-layer thickness isopach [from *Hogg and Stommel*, 1985], and the boundary current streamline is deduced from water sample data [see *Pickart*, 1987]. (*b*) The streamlines of the numerical model, meant to represent the circulation in Figure 3*a*. The domain is 2000 × 1000 km with a grid spacing of 25 km.

portion of the plume which spreads inward encounters a region of stronger velocity and advects around more quickly. Note also that the spiral is asymmetric in that where the flow is zonal the spiral is not as pronounced as in the meridional flow. To understand why this asymmetry exists, it must be understood what factors govern the spiral. To do this, a problem involving diffusion in a simple shear flow is considered.

The effect that velocity shear has on the spreading of a passive tracer has been studied considerably, particularly the process of shear dispersion whereby cross-stream shear enhances the spreading of tracer along streamlines [*Rhines*,

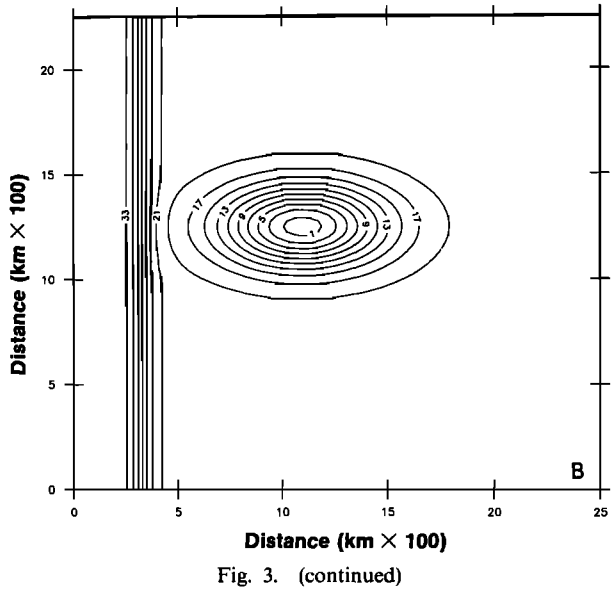

Fig. 3. (continued)

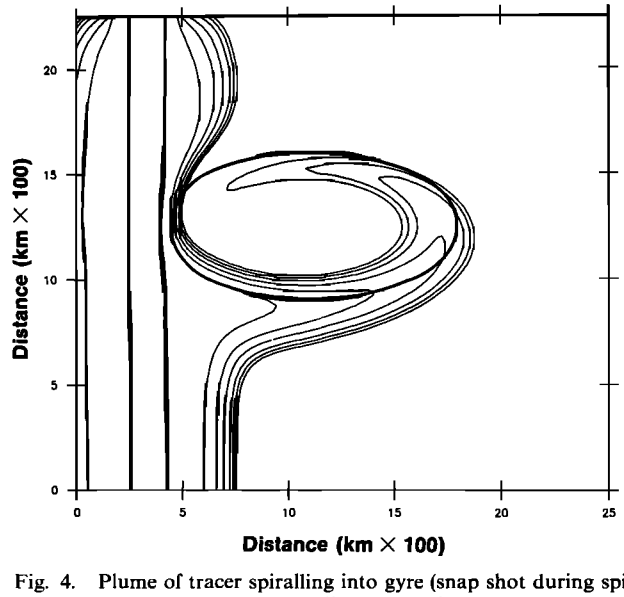

Fig. 4. Plume of tracer spiralling into gyre (snap shot during spin up). The dark lines are the bounding streamlines of the gyre and boundary current.

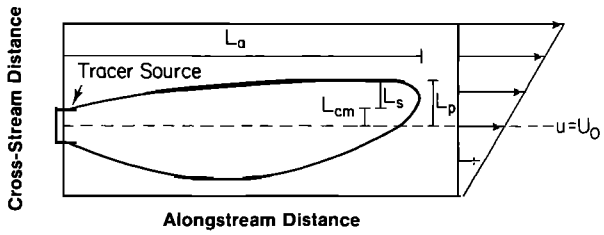

Fig. 5. Depiction of a plume of tracer in a linear shear flow. Length scales of the plume are as shown; tracer is input at $u = U_0$.

1983]. Here we address a different aspect in which cross-stream shear influences the diffusion of tracer.

For a given distribution of tracer consider the parameter which is the ratio of the alongstream gradient to the cross-stream gradient, $\theta_x/\theta_y = \delta_L$. The value of δ_L is one measure of the extent to which shear dispersion occurs. For the same shear and diffusivity a large δ_L means prevalent shear dispersion, whereas a small δ_L means this effect is negligible. Shear dispersion acts on a distribution of tracer to reduce its δ_L [*Rhines*, 1983].

Here we are interested in the effect that cross-stream shear has on the spreading of tracer across streamlines, when the distribution of tracer is characterized by a small δ_L, i.e., a tracer plume. The analysis applies to situations in which there is a localized source of tracer. Such a distribution in a linear shear flow is analogous to the plume of tracer penetrating the edge of the gyre.

3.1. *Linear Shear Flow*

Consider the advective-diffusive problem schematically illustrated in Figure 5, which is designed to isolate the mechanism by which tracer enters the gyre in the model. At $t = 0$ a step function source is turned on, and tracer progresses downstream while spreading laterally. The center of mass of the tongue proceeds to migrate across streamlines as with the gyre flow. It is relevant to define four length scales for this problem:

L_p, the cross-stream penetration of tracer. At each location alongstream the cross-stream extent of the plume is defined as the distance to a given percent concentration (say the e-folding concentration) of the local plume amplitude at that location. L_p is the maximum such penetration.

L_a, the alongstream length of the tongue, which is defined as the zonal distance to where the meridional penetration is greatest.

L_{cm}, the displacement of the center of mass of the tongue across streamlines at the point where the meridional penetration is greatest. This measures migration of the tongue. (Note that migration requires cross-stream shear.)

$L_s = L_p - L_{cm}$; this measures spreading of the tongue.

The quantities L_a and L_p are the x and y length scales of the tracer distribution; L_{cm} and L_s are the first and second y moments (Figure 5). For a northward diffusing particle of tracer, consider the balance between advection and diffusion where $u = U_0 + \alpha y (v = 0)$,

$$(U_0 + \alpha y)\theta_x = \kappa\theta_{xx} + \kappa\theta_{yy} \tag{2}$$

where U_0 = (constant) reference velocity, and α = cross-stream shear.

We estimate the order of magnitude of each term in (2) using the x and y length scales and define the following nondimensional parameters: the aspect ratio $\delta = L_p/L_a$; the alongstream Peclet number $P_a = (U_0 + \alpha L_p)L_a/\kappa$, which is the alongstream diffusive time scale divided by the advective time scale; and the cross-stream Peclet number $P_c = P_a\delta^2$, which is the cross-stream diffusive time scale divided by the advective time scale.

In terms of these parameters the balance in (2) becomes

$$P_a\delta^2 \sim \delta^2 + 1 \tag{3}$$

3.1.1. *Large alongstream Peclet number: Relationships between length scales.* Consider first the limit of small diffusivity and small aspect ratio ($\delta \ll 1$), where $P_a \gg 1$ but P_c remains O(1). The dominant balance in (3) is

$$P_a\delta^2 \sim 1 \tag{4}$$

Note that the alongstream Peclet number P_a is composed of two parts, which can be thought of as two separate alongstream Peclet numbers: one for the shear part of the flow and one for the uniform part (the reference velocity). We define the parameter S as the ratio of these two Peclet numbers, which is a measure of the shear that the tracer experiences, $S = \alpha L_p/U_0$. With this, (4) can be rewritten

$$1 + S \sim \frac{\kappa}{L_a U_0 \delta^2}$$

In the limit $S \ll 1$ the shear is negligible and L_p obeys the rule

$$L_p \sim \left(\frac{\kappa L_a}{U_0}\right)^{1/2} \tag{5}$$

In the opposite limit, $S \gg 1$, the shear is so strong that the reference velocity is negligible. Here L_p obeys the rule

$$L_p \sim \left(\frac{\kappa L_a}{\alpha}\right)^{1/3} \tag{6}$$

When $S \sim 1$, the shear and the reference velocity are comparable, and $L_p \sim U_0/\alpha$.

Three different examples of distributions in which $P_a \gg 1$, $P_c \sim 1$ appear in Figure 6. (The solutions were obtained numerically using the scheme described above, with appropriate boundary conditions.) Each example represents a snapshot as the tongue of tracer evolves. In the first ($S \ll 1$)

$$S = 0.1 \qquad L_p \sim L_s \gg L_{cm}$$

In the second ($S \gg 1$)

$$S = 2.3 \qquad L_p \sim L_{cm} \gg L_s$$

In the third

$$S = 0.6 \qquad L_p > L_{cm} \sim L_s$$

(A complete listing of parameters appears in Table 1.) As the plume in the first example progresses downstream, L_p follows the $S \ll 1$ law, and in the second example it follows the $S \gg 1$ law (Figures 7*a* and 7*b*). In the former, where the shear is negligible, one would expect the tongue to spread in the same way as the envelope traced out by a spot of dye progressing downstream from the origin. The width of such a dye spot increases with downstream distance as $2(\kappa x/u)^{1/2}$, which agrees with (5) and gives the slope of 1/2 obtained from Figure 7*a*. In the third example, L_p corresponds to neither of these laws; its slope is between the values of 1/2 and 1/3 (Figure 7*c*).

When the shear is negligible, spreading of the tongue ac-

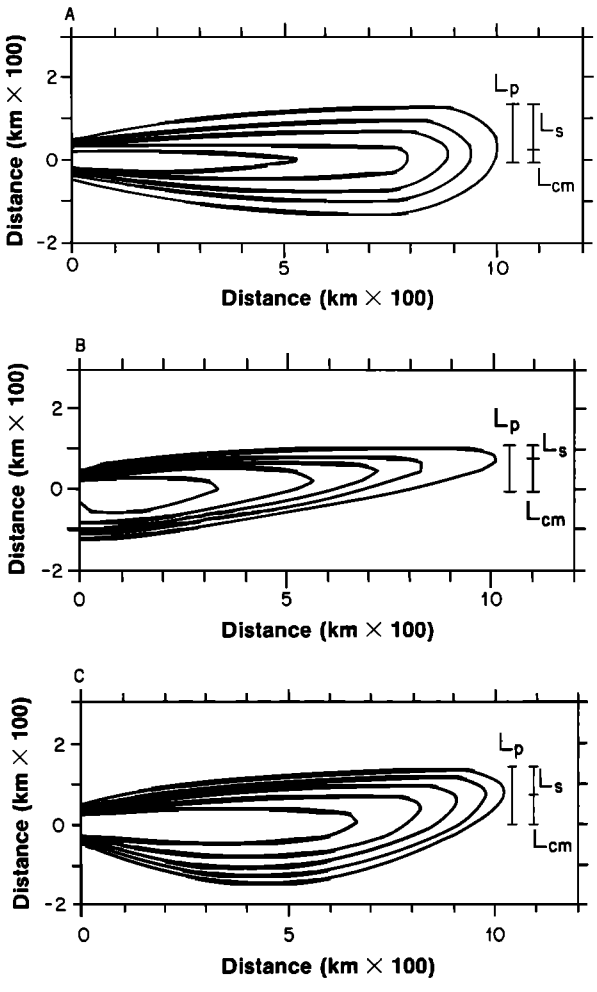

Fig. 6. Snap shot of tracer in which $P_a \gg 1$, $P_c \sim 1$. (*a*) $S = 0.1$, which corresponds to spreading, (*b*) $S = 2.3$, which corresponds to migration, (*c*) $S = 0.6$, which is between the limits of spreading and migration.

counts for most of the penetration of tracer across streamlines. In a strongly sheared flow, however, the penetration is mostly due to migration of the tongue. In the third example, which is between these extremes, spreading and migration are both substantial; however, with increasing penetration the shear extreme is approached, and correspondingly, L_{cm} becomes more closely correlated with L_p. Note that this example does not correspond exactly to the $S \sim 1$ case discussed above, which implies that when U_0 and αy are of equal magnitude, spreading and migration will not contribute equally to the penetration but rather migration will be somewhat more prevalent.

TABLE 1. Parameters for the Different Examples of the Linear Shear Problem

Figure	S	P_a	α, cm/s/ (km × 100)	U_0, cm/s	L_p, km × 100
6*a*	0.1	7.7	0.5	5.0	1.4
6*b*	2.3	7.6	4.0	2.0	1.2
6*c*	0.6	7.5	1.5	3.5	1.4
8*a*	1.1	10.4	2.0	3.0	1.6
8*b*	1.2	0.2	0.3	0.5	2.0

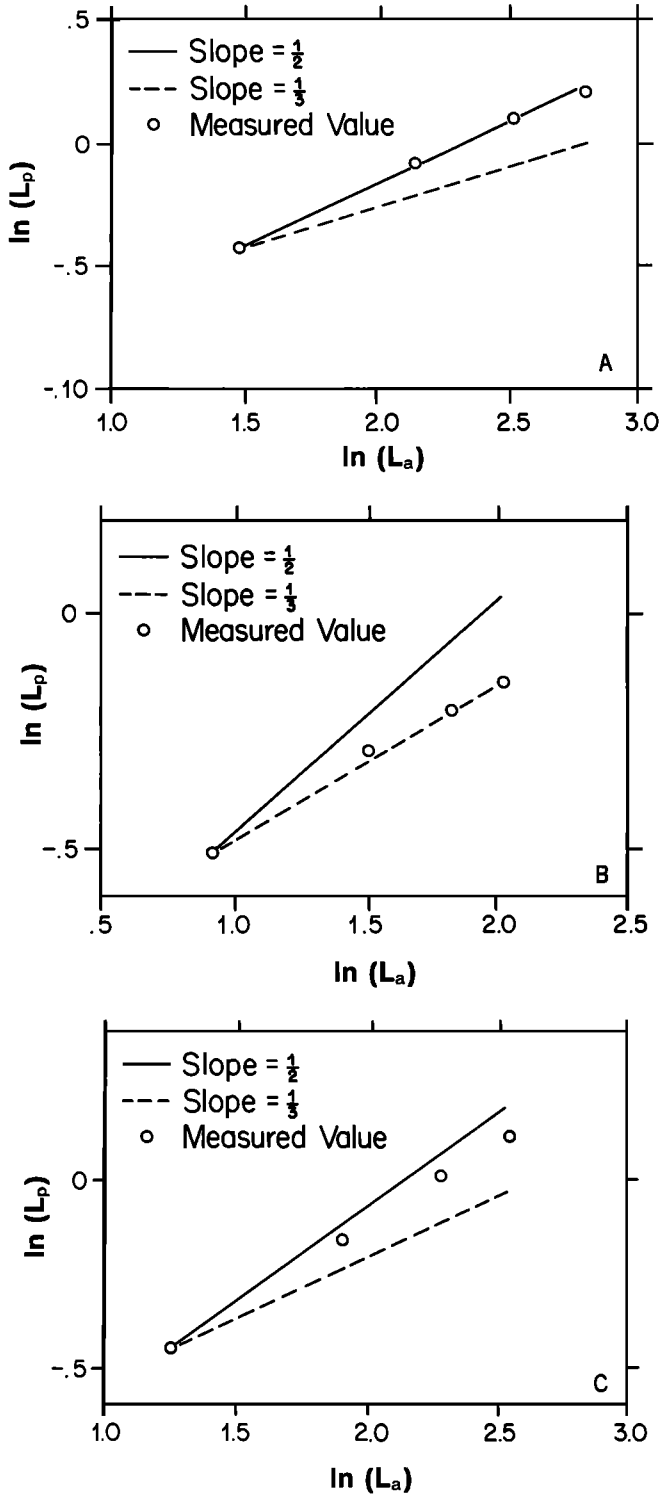

Fig. 7. Relationship between the x and y length scales of the plumes in Figure 6 at four successive times. A slope equal to one half is consistent with (5); a slope equal to one-third is consistent with (6). (*a*) For the plume of Figure 6*a*, (*b*) For the plume of Figure 6*b*, (*c*) For the plume of Figure 6*c*.

These results can be obtained analytically as well through an analysis of a slightly different (simpler) problem: that of a point drop of dye in a linear shear flow. *Smith* [1982] solved this case, and while the dye drop is not a continuous source but rather an initial distribution that evolves, the same infor-

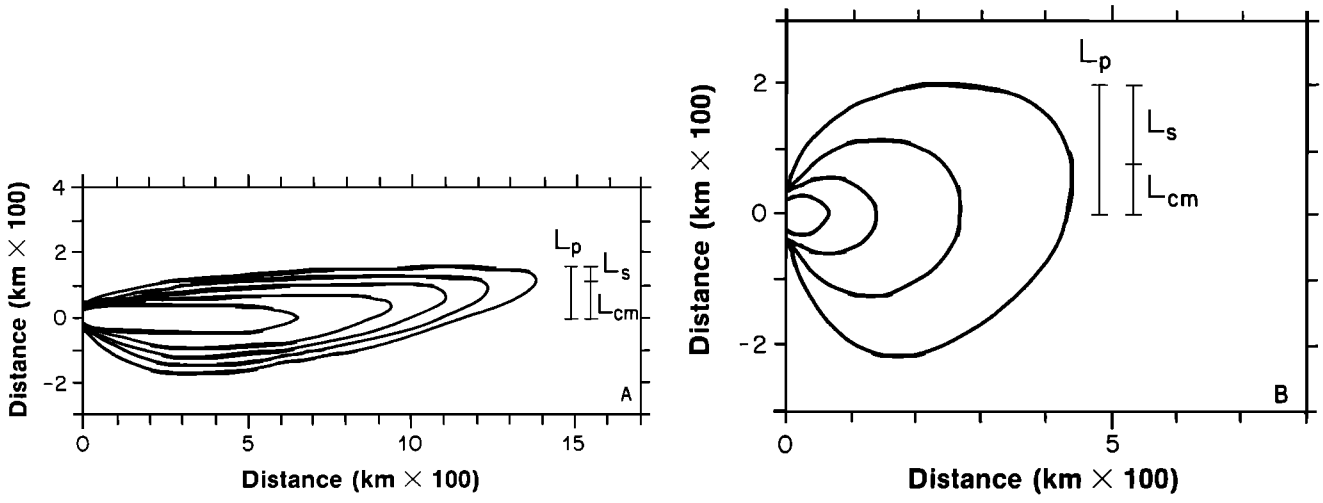

Fig. 8. (*a*) Snap shot of tracer in which $P_a \gg 1$, $P_c \sim 1$ with a value of S such that migration is more prevalent than spreading. (*b*) $P_a \ll 1$, $P_c \ll 1$ in which spreading is more prevalent than migration for a comparable value of S.

mation regarding penetration can be derived [see *Pickart*, 1987]. Because of its similarity to the gyre problem however the continuous source problem was examined here.

3.1.2. *Small alongstream Peclet number: Enhancement of Spreading.* In the first set of examples (Figure 6) it is seen that for $S \gg 1$, migration of the plume, i.e., movement of its center of mass is more prevalent than spreading, and for $S \ll 1$ the opposite is true. In each of these cases, $P_a \gg 1$. With a smaller P_a the system becomes less sensitive to the velocity and, more importantly, to changes in the velocity. Thus we might expect that a smaller P_a will diminish the importance of migration versus spreading, as is the case with a small S. The distinction between $S \ll 1$ and $P_a \ll 1$ should remain clear, however: In the first instance the cross-stream change in velocity is unimportant because it is small, and in the second instance it is unimportant because the system does not detect it.

A second set of examples appears in Figure 8. In Figure 8*a*, $P_a \sim 10$, and in Figure 8*b*, $P_a \sim 0.1$ (S is comparable in each; see Table 1). Indeed, with a large alongstream Peclet number, $L_{cm} > L_s$, whereas with a small alongstream Peclet number, $L_s > L_{cm}$. Note, however, that in Figure 8*b*, $L_p \sim L_a$, so that the balance of terms in (4) is not applicable here, i.e., the aspect ratio is now O(1) and the alongstream diffusive term must be retained. In this case, both the alongstream and cross-stream Peclet numbers are small, whereas previously $P_a \gg 1$ and $P_c \sim 1$. The dominant balance in (3) for this example is $-\delta^2 \sim 1$.

3.1.3. *Cross-stream penetration.* It is seen that variation in the alongstream Peclet number P_a alters the importance of alongstream diffusion versus advection in balancing the cross-stream diffusion. Variation in the shear parameter S enhances or diminishes advection by a constant velocity versus a sheared velocity. This means that two criteria must be satisfied in order to obtain migration of the tracer plume. First, P_a must be large enough so that the system is sensitive to the velocity field (this condition is necessary but not sufficient). In addition, S must be large enough that the cross-stream shear is significant.

As an alternative to L_p as a measure of cross-stream penetration, consider the integral of tracer in the region $y > 0$, $x < L_a$, i.e., the total amount of tracer that has penetrated northward. Here lies a further distinction between $S \gg 1$ and $S \ll 1$. For two plumes, one in a strongly sheared flow and one in a uniform flow, in which L_a and L_p are the same there is significantly less tracer north of $y = 0$ in the sheared flow. This is because the northward shear increases the northward gradient of tracer, and this causes a southward flux of tracer across part of the $y = 0$ line. Thus although tracer has penetrated just as far across-stream in the sheared flow, there is less of it.

Although the $P_a \ll 1$ limit resembles that of $P_a \gg 1$, $S \ll 1$ in that spreading of the plume is more prevalent than migration, these instances represent opposite extremes in penetration. For a specified flow field (U_0 and α) and a given L_a the value of L_p depends on κ. A sufficiently small κ means that L_p is too small for the plume to sense the shear, and large P_a spreading occurs. For larger κ (and L_p) the $S \gg 1$ limit is approached and migration becomes important. Small P_a spreading occurs with even larger κ, and this represents the upper extreme of penetration.

3.2. *Application to Gyre Flow*

We return now to the gyre problem. The process by which the plume of tracer penetrates the edge of the gyre and diffuses into a region of stronger flow resembles the shear flow problem analyzed above, and some of the ideas previously developed are applied now to this problem. There are differences, however, between the two problems. Here the cross-stream shear α varies both alongstream and across-stream, alongstream shear is present as well, the flow is curved rather than rectilinear, and the input of tracer to the gyre is not a step function in time.

Figure 9 shows a time history of tracer penetrating the gyre. The advancement of the plume in each one-year segment can be thought of as a separate example of the shear flow problem examined above, with the following definitions: L_a, the distance that the leading edge of the plume travels alongstream in a year, L_{cm}, movement of the center of mass of the leading edge of the plume across-stream in a year, α, cross-stream shear halfway between the source and the leading edge of the plume (the alongstream shear is negligible with respect to α), and U_0, velocity at the source.

These quantities are analogous to those similarly named in the previous shear flow problem. The gaussian at the up-

stream edge of the boundary current is a step function applied at $t = 0$, but by the time tracer reaches the gyre it is no longer characterized by a sharp front, i.e., the source for each of the above examples grows in amplitude and width. This means we are unable to define the analog to L_p, which in turn means we are unable to measure directly the values P_a and S. We can, however, estimate the size of P_a by noting that δ, the aspect ratio, is much less than one for each one-year segment (Figure 9), and this implies that $P_a \gg 1$. The first condition for migration is thus satisfied everywhere around the gyre.

Because a spiral does occur, it is natural to assume that the second condition for migration, $S \gg 1$, is satisfied as well. Recall that in this limit, $L_p \sim L_{cm}$. Since we can measure L_{cm}, we are then able to check this assertion. For each single-year segment we substitute the values of α, L_a, and κ into (6), where L_p is replaced by L_{cm} (the proportionality constant for (6) was determined numerically). This predicted value of L_{cm} is in turn compared to the measured value. The results of this comparison (Figure 10) show that there is good agreement between the predicted and measured values where the flow is meridional. However, while the predicted curve does show smaller penetration in the zonal flow, it is still significantly more than what actually occurs, suggesting that the migration limit does not apply in the zonal flow.

Figure 11 graphs the values of U_0 and α which the plume experience as it travels around the gyre. Also shown is the extent of the corresponding spiral. The fact that both α and U_0 are larger in the zonal flow, together with the small extent of migration there, suggests that this corresponds to the advective limit. In particular, in these regions not only is $P_a \gg 1$, but $P_c \gg 1$ as well so that isolines of tracer nearly coincide with streamlines. It is more accurate then to think of the plume as mirroring streamlines when it travels in the stronger zonal flow, while spiraling across streamlines in the manner of the above shear flow problem when it travels in the weaker meridional flow.

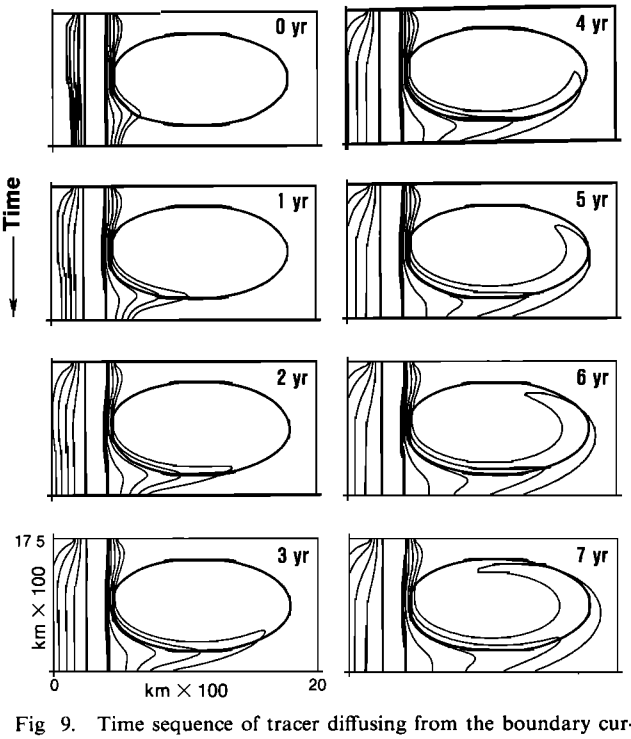

Fig 9. Time sequence of tracer diffusing from the boundary current and becoming entrained into the gyre. The dark lines are the bounding streamlines.

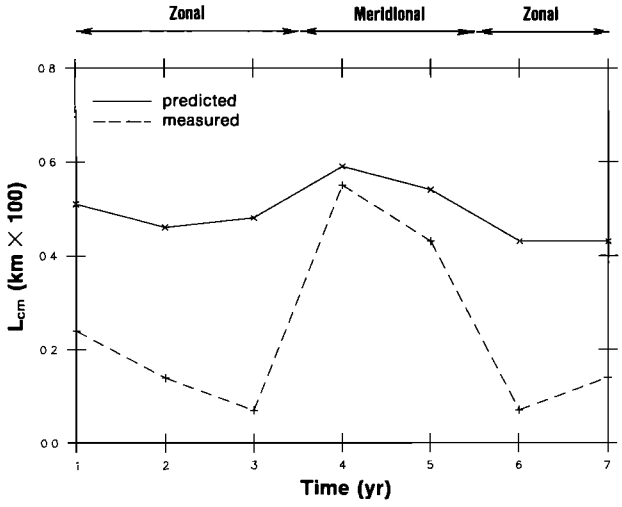

Fig. 10. Comparison of L_{cm} as measured from successive distributions of Figure 9, versus the value predicted from (6). The plume's direction of travel is indicated above.

4. HOMOGENIZATION

As the gyre simulation progresses to steady state, the tracer in the center part of the gyre becomes uniformly distributed. This occurrence of homogenization is related to the penetration process described above. Before proceeding with a discussion of this problem we first review the argument for homogenization following *Rhines and Young* [1982*a*].

4.1. *Review of Homogenization*

Consider the steady state balance of advection and diffusion in a gyre, governed by the steady form of (1),

$$\mathbf{u} \cdot \nabla\theta = \nabla \cdot \kappa\nabla\theta$$

Integrating over the area bounded by a streamline and applying the divergence theorem gives,

$$\int_s \mathbf{u}\theta \cdot \mathbf{n}ds = \int_s \kappa\nabla\theta \cdot \mathbf{n}ds \tag{7}$$

where S is the bounding streamline and $\mathbf{n}$ is the unit normal to the streamline. Note that the left-hand side of (7) is identically zero because $\mathbf{u}$ and $\mathbf{n}$ are perpendicular.

In the limit of strong advection/weak diffusion, isolines of tracer nearly coincide with streamlines, i.e., $\theta = \theta(\psi)$. This gives

$$\nabla\theta = \theta(\psi)_\psi \nabla\psi$$

and since the integral is around a streamline,

$$\theta(\psi)_\psi \int_s \kappa\nabla\psi \cdot \mathbf{n}ds = 0$$

The quantity inside the integral is positive definite, which further implies that

$$\theta(\psi)_\psi = 0 \qquad \theta = \text{const}$$

Homogenization is thus obtained in a strongly advective system.

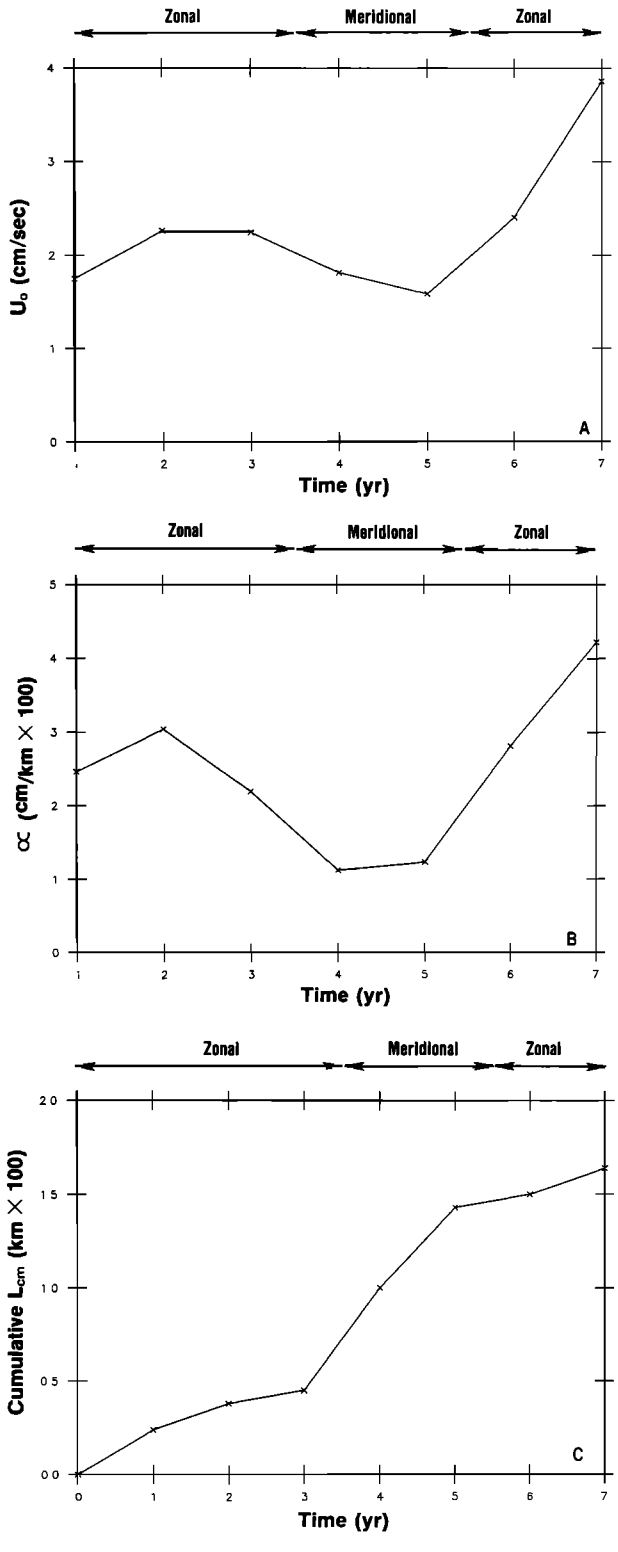

Fig. 11. (*a*) The value of the reference velocity for the distributions of Figure 9. (*b*) The value of the cross-stream shear. (*c*) The cumulative migration of the plume.

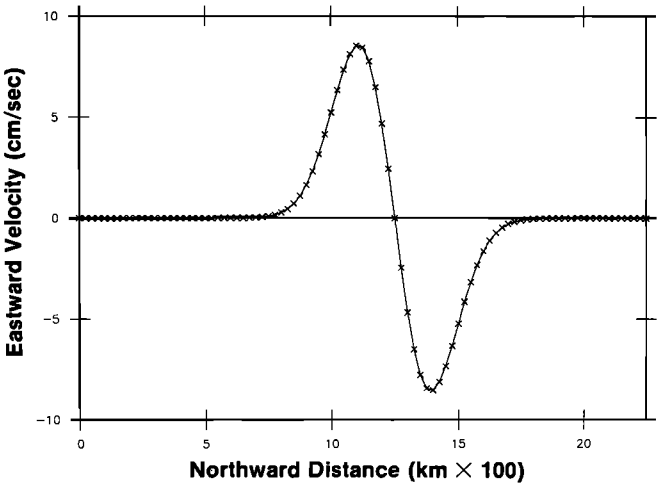

Fig. 12. North-south velocity section through the center of the gyre of Figure 3*b*.

4.2. *Spatially Decaying Gyre*

The flow field that *Musgrave* [1985] used in his numerical study of homogenization consisted of Stommel-type gyre, in which the strongest flow occurs at the edge of the gyre. He defined a Peclet number, $P = UL/\kappa$, using the length scale of the basin (L) and the characteristic velocity of the gyre (U) and discussed the extent of the homogeneous pool versus P. In terms of (1) the Peclet number determines to what extent advection balances diffusion and L should be defined in terms of the tracer distribution. It is unclear how to discuss results in terms of a Peclet number so defined, especially with regard to homogenization when locally the length scale becomes infinite. Here we define P in terms of the plume of tracer which penetrates the gyre, as was done in the previous section.

The gyre presently being considered has its maximum velocity relatively close to the center, decaying from this point to the edge (Figure 12). For simplicity, for the time being we consider an axisymmetric, i.e., circular gyre. We divide the gyre into two regions: the edge where the flow is weak and the inner part where the flow is more intense (close to the gyre center the flow once again becomes weak).

As the plume of tracer enters the outer, weaker part of the flow, it spirals across streamlines (provided the shear is strong enough) in the manner discussed above. This region is characterized by $P_a \gg 1$, $P_c \sim 1$. Eventually, the plume reaches

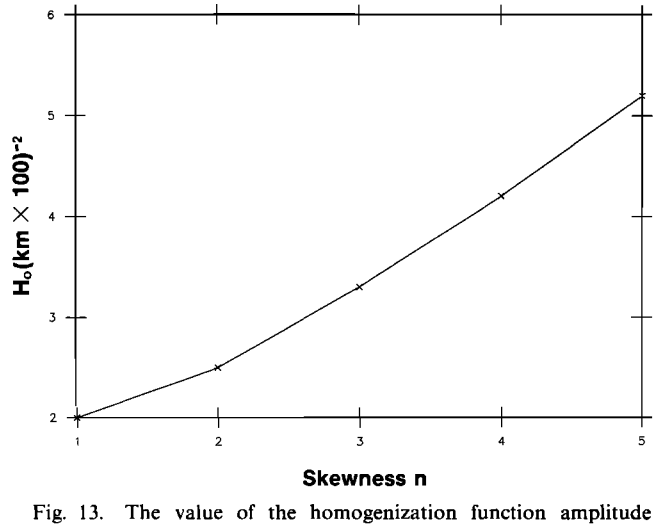

Fig. 13. The value of the homogenization function amplitude versus the skewness of a gyre. The skewness n is defined as the ratio of the major axis of the ellipse to the minor axis. The area of the gyre is the same in each case and set equal to π.

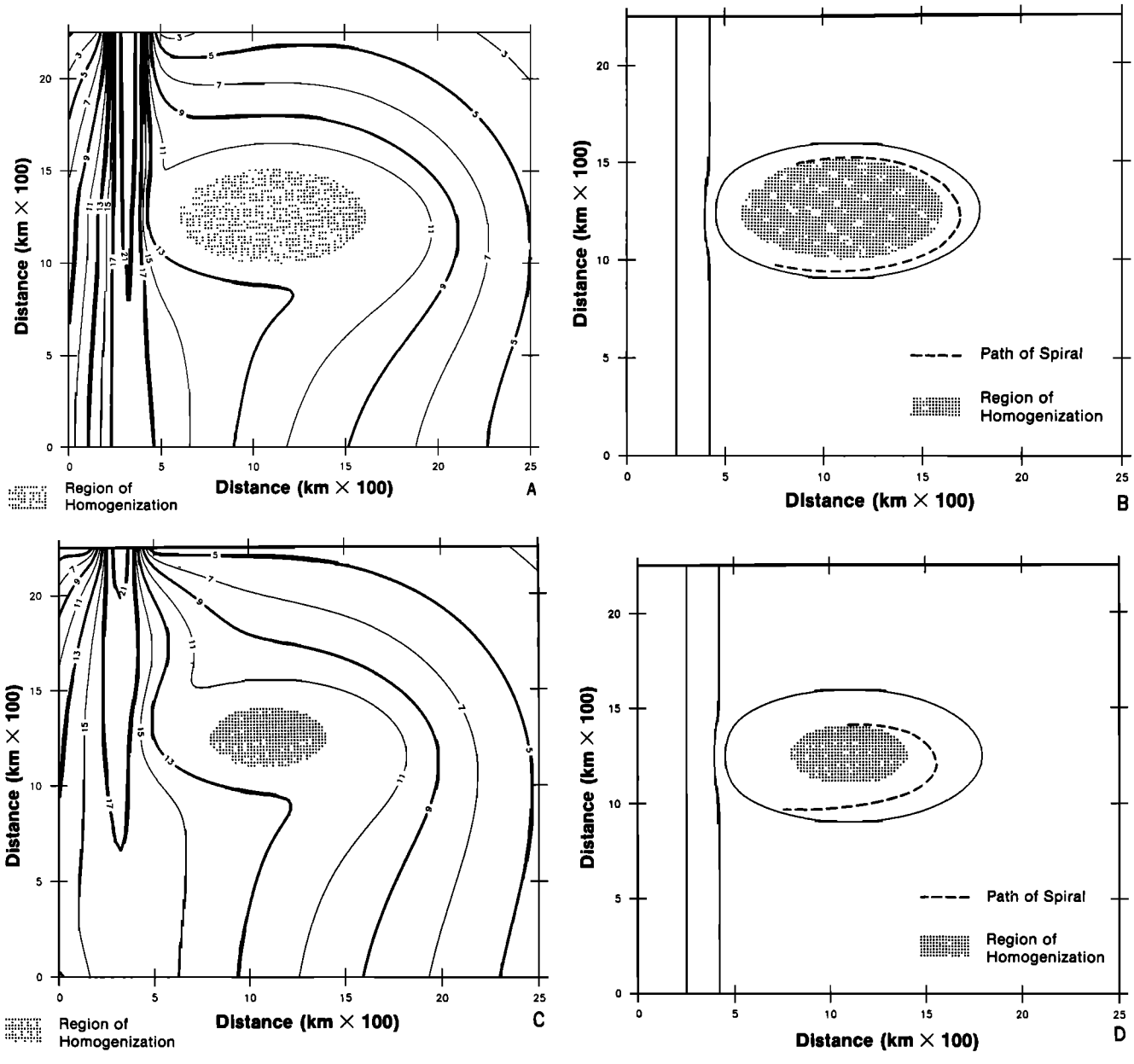

Fig. 14. (*a*) Steady state distribution of tracer for $\kappa \sim 10^6$ cm^2/s. The shaded region corresponds to the area of the gyre in which the gradient of tracer is < 0.1 concentration units/(km × 100). This is taken as the criterion for homogenization. (*b*) The region of homogenization in Figure 14*a* shown in relation to the inward spiral of the plume of tracer during spin up. The solid lines are bounding streamlines. (*c*) Steady state distribution for $\kappa \sim 5 \times 10^6$ cm^2/s. (*d*) Homogenized region and spiral for $\kappa \sim 5 \times 10^6$ cm^2/s.

strong enough flow (we clarify below what is meant by strong enough) that it is nearly pulled around a streamline. At this point the spiral has "collapsed" to a streamline, and here $P_a \gg 1, P_c \gg 1$. As discussed above, these latter conditions describe the advective limit, which is the necessary condition for homogenization. Specifically then, the outer region of the gyre is where the spiral occurs, and the inner region, delimited by the collapsed spiral, is where homogenization occurs.

For the nonaxisymmetric gyre we saw above that as the plume first enters the gyre progressing eastward, the fast flow keeps it nearly confined to a streamline. However, when the plume turns northward, the flow along that same streamline weakens and the plume proceeds to spiral significantly inward. In this case, the division between the two regions of the gyre is not as clear cut. However, homogenization will not occur until the plume tracks a streamline around an entire circuit. Thus even though portions of the spiral may collapse, it is only where the cumulative spiral collapses that the transition occurs between the two regions.

We now examine more closely the condition that the flow be strong enough to keep the plume from diffusing appreciably across-stream in the time it takes to recirculate. The advective limit is given by $P_a \gg 1$ and $P_c \gg 1$. The more stringent of these is $P_c \gg 1$, which, by definition, implies that

$$P_c = \left(\frac{U}{L_a}\right)\left(\frac{L_p^2}{\kappa}\right) \gg 1$$

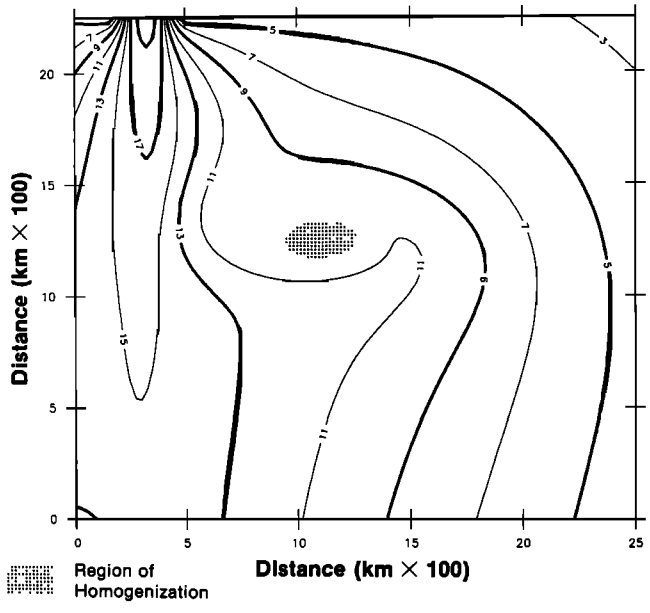

Fig. 15. Steady state distribution for $\kappa \sim 10^7$ cm^2/s.

For a circuit around the gyre the relevant length scale is $L_a = L_s$, the perimeter of the streamline, and the relevant velocity scale is $U = \bar{v}_s$, the average velocity around the streamline. We define the homogenization function H as the ratio of these two quantities, which gives

$$P_c = H(\psi)\left(\frac{L_p^2}{\kappa}\right)$$

where $H(\psi) = \bar{v}_s(\psi)/L_s(\psi)$. The function H, which is the inverse of the circulation time, can be thought of as a measure of the tendency for homogenization to occur based only on flow characteristics. A larger H means greater likelihood for homogenization.

Consider again the axisymmetric gyre, whose streamfunction is given by

$$\psi = \psi_0\left(1 - e\,\frac{-r^2}{L^2}\right) \tag{8}$$

where ψ_0 is the amplitude, and L is the e-folding length scale of the gyre. In this case, $\bar{v}_s = v_s$. From (8),

$$v_s = \frac{\partial\psi}{\partial r} = \frac{2}{L^2}(\psi_0 - \psi)r$$

The perimeter $L_s = 2\pi r$, which gives

$$H(\psi) = \frac{1}{\pi L^2}(\psi_0 - \psi)$$

This says that the greatest tendency for homogenization is at the gyre center, decreasing linearly with increasing ψ. Thus the innermost part of the gyre, where the flow becomes weak again, is included in the advective region because the circulation time is small (the perimeter of a streamline is small). Contrast this to solid body rotation, $\psi = \psi_0 r^2$, where the circulation time is constant for each streamline. Here $v_s = 2\psi_0 r$ and $H(\psi) = \psi_0/\pi$; thus the tendency for homogenization is the same everywhere.

In the nonaxisymmetric gyre the velocity along a streamline varies around the gyre. The streamfunction is

$$\psi = \psi_0\left[1 - \exp\left(\frac{-x^2}{L_x^2} - \frac{-y^2}{L_y^2}\right)\right] \tag{9}$$

where L_x and L_y are the x and y e-folding length scales. Note that

$$H = \frac{\bar{v}_s}{L_s} = \frac{\dfrac{1}{L_s}\displaystyle\int_S \mathbf{u}\cdot d\mathbf{s}}{L_s} = \frac{\Gamma}{L_s^2}$$

where Γ is the circulation around the streamline S. From (9),

$$\Gamma = 2\pi\psi_0\left(\frac{L_x^2 + L_y^2}{L_x L_y}\right)\left(1 - \frac{\psi}{\psi_0}\right)\ln\left(1 - \frac{\psi}{\psi_0}\right)^{-1}$$

$$L_s^2 = 4\pi^2 L_x L_y \ln\left(1 - \frac{\psi}{\psi_0}\right)^{-1}$$

which gives

$$H(\psi) = \frac{H_0}{2\pi}(\psi_0 - \psi) \tag{10}$$

where $H_0 = (L_x^2 + L_y^2)/(L_x L_y)$. Figure 13 graphs H_0 as a function of gyre skewness. It shows that for a given value of ψ, homogenization is more likely to occur in a more skewed gyre. Note that this is true even though the velocity at the two widest sections of the gyre approaches zero as the gyre's skewness increases (the portion of the streamline in these sections gets vanishingly small as well).

4.3. *Limits of Diffusivity*

Homogenization within the asymmetric gyre of Figure 3 was examined versus various values of the diffusivity κ. The smallest value considered was $\kappa \sim 10^6$ cm^2/s, and the homogeneous pool of tracer that formed in steady state is shown in Figure 14*a*. This is the final state of the example analyzed above in terms of the asymmetric spiral. Figure 14*b* shows the path of the spiral and how it closes in on the region which eventually becomes homogenized.

When the diffusivity is increased to $\kappa \sim 5 \times 10^6$ cm^2/s (for the same gyre), this in effect causes the flow to appear weaker to the incoming plume of tracer. As a result, the zonal flow no longer corresponds to the advective limit, so a pronounced spiral occurs there as well as in the meridional flow, i.e., the asymmetry no longer exists (Figure 14*d*). Consistent with (10), the plume now has to penetrate further into the gyre before it encounters flow strong enough to induce homogenization. Correspondingly, the size of the steady state homogenous pool is reduced (Figure 14*c*).

Upon increasing κ further ($\kappa \sim 10^7$ cm^2/s), a transition occurs in the manner in which tracer fills the gyre. The diffusivity is so large that the meridional flow (which is weaker than the zonal flow) is essentially "turned off," i.e., the diffusive flux is now on the order of the advective flux. Thus when the plume of tracer turns northward in the gyre it stagnates. By the time tracer diffuses northward from there and gets caught in the zonal flow and advected westward the westward diffusing tracer from the stagnation point has penetrated the center of the gyre. So whereas in the previous two cases, tracer was advected completely around the gyre and filled the gyre center in a bowllike fashion, here it is advected to the east and then proceeds to fill the gyre from east to west. Figure 16 contrasts the penetration of tracer into the gyre for the various values of

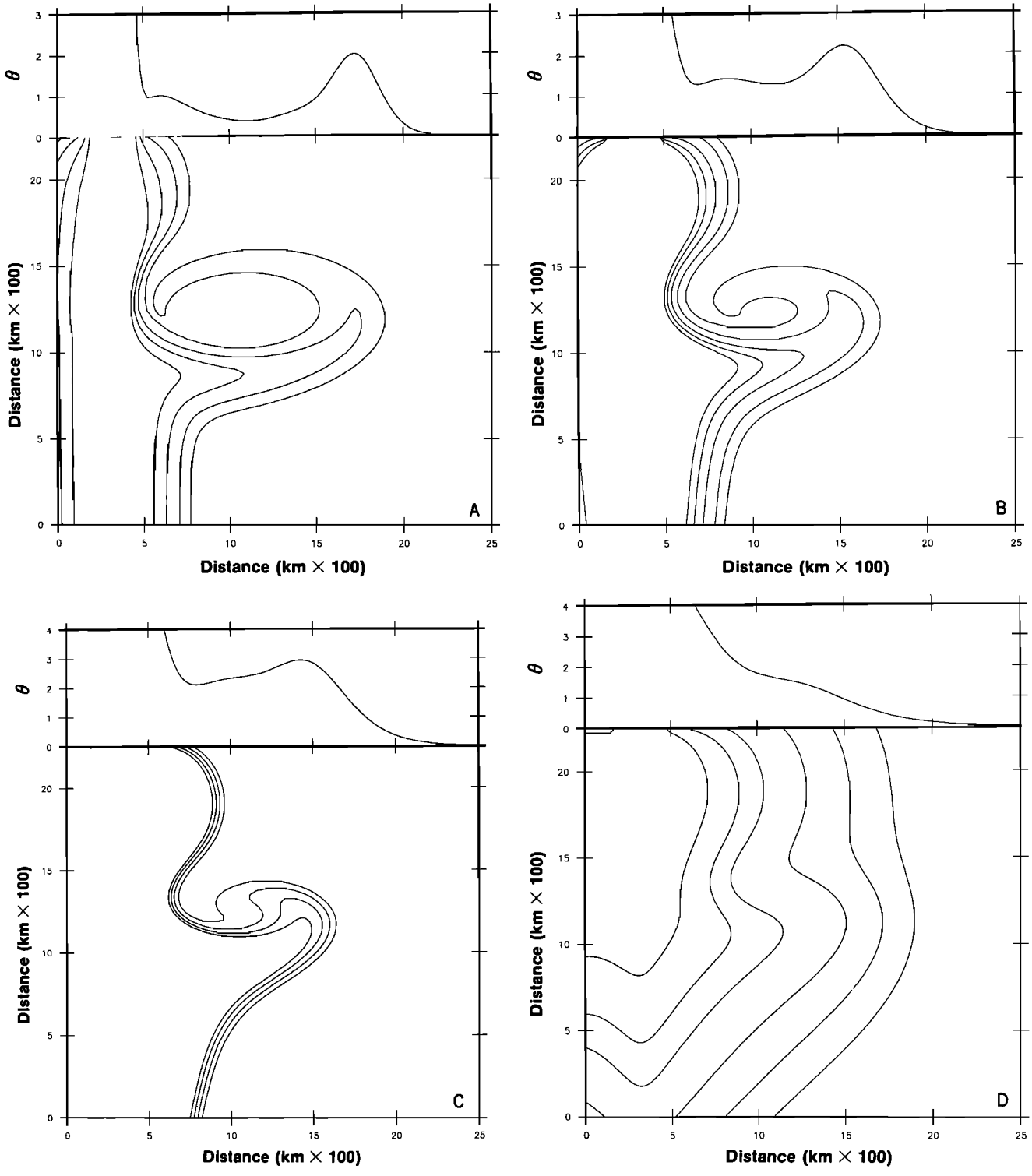

Fig. 16. Snap shot of tracer during spin up illustrating the manner in which tracer fills the gyre. Shown above is a zonal section through the center of the gyre. (*a*) $\kappa \sim 10^6$ cm^2/s. (*b*) $\kappa \sim 5 \times 10^6$ cm^2/s. (*c*) $\kappa \sim 10^7$ cm^2/s. (*d*) $\kappa \sim 5 \times 10^7$ cm^2/s.

diffusivity. A small amount of homogenization does occur at the center of the gyre (Figure 15).

The final case considered can be thought of as the diffusive limit ($\kappa \sim 5 \times 10^7$ cm^2/s). Here the presence of the zonal flow is hardly felt as well, and the manner in which the gyre is filled undergoes yet another change. As shown in Figure 16, tracer diffuses from west to east across the gyre, with an undulation corresponding to the eastward and westward flows.

5. SUMMARY

The preceding analysis examined the entrainment and homogenization of tracer in a gyre which initially was tracer-free. The entrainment is characterized by a plume of tracer spiraling asymmetrically inward across streamlines as a result of the cross-stream shear. In particular, in the zonal flow the spiral is minimal as the strong flow causes the plume to follow stream-

lines. In the meridional flow the spiral is of considerable extent, conforming to the ideas developed in a simpler shear flow analysis.

Previous work has been done on the mixing of tracers within a subtropical gyre. *Musgrave* [1985] analyzed steady state numerical solutions in which the northern boundary is maintained at a uniform positive concentration while the southern boundary is kept uniformly negative. He discussed the presence of a spiral that extends from the boundary to the stagnation point of the flow at the center of the gyre. This spiral arises, however, because of the choice of boundary conditions (the cross-stream shear of the gyre is of the wrong sense to cause the type of spiral discussed here, i.e., α is everywhere < 0). As tracer enters from the northern boundary, it travels anticyclonically and spreads into the interior. Upon encountering the negative plume that extends from the south the region of positive concentration shifts away from the boundary, hence the spiral. For the type of gyre considered here the inward extent of the spiral depends on the flow parameters and diffusivity. (The maximum distance over which the spiral can extend is to the region where the cross-stream shear vanishes.)

Homogenization is the steady state manifestation of tracer penetrating a closed circulation, provided the system is strongly advective. For the spatially decaying gyre considered here the occurrence of homogenization is closely tied to the characteristics of the spiraling plume of tracer which forms during spin-up. In particular, where the spiral collapses to a streamline marks the outer extent of the homogeneous pool that eventually develops. As the diffusivity is increased, the size of this pool shrinks. This is consistent with the idea that homogenization occurs more readily nearer the center the gyre for this type of flow, based on the shorter circulation times there.

APPENDIX: THE OPEN DIFFUSIVE BOUNDARY CONDITION

The advective-diffusive numerical model is a regional model designed to examine a subbasin scale problem with high resolution and small implicit diffusion. Consequently, the boundaries of the model correspond to open ocean, and the task of applying the boundary conditions is not straightforward. Save for the small region of inflow and outflow at the ends of the boundary current the flow at the edge of the domain is negligibly small. The velocities here were made identically zero so that only diffusion at the boundary need be addressed.

The centered-differencing scheme used for diffusion in the model interior is not applicable at the boundary. A boundary scheme was developed in which the concentration of tracer there evolves in time in a manner simulating diffusion. This enables tracer to diffuse out of the domain.

The criterion used to specify the boundary concentration consists of an extrapolation repeated at each time step. The basis for the idea is that, as the simulation progresses, tracer accumulates within the domain and proceeds to flux outward through this part of the boundary. More specifically, the gradient of tracer normal to the open boundary is always inward (except initially when it is zero). We thus use what is known about the flux of tracer just inside the boundary. In particular, we compute the trend of outward flux as the boundary is approached, extrapolate this trend, and then apply it at the boundary.

This is the substance of the boundary scheme. Rather than use the value of flux, however, a different quantity is extrapolated which is the ratio of successive concentrations along the outward normal (rather than the difference). This results in better simulation of the smoothing properties of diffusion [see *Pickart*, 1987]. At each time step then the interior solution is determined using the finite difference scheme; then the above mentioned trend is computed at each location along the boundary, from which the boundary concentration is determined.

The details of this are as follows. Let θ_i represent the value of tracer at grid point i along an outward normal to the boundary, and θ_{i+1} be its adjacent value towards the interior of the domain ($i = 1$ denotes the first value inside the boundary). We define the parameter $R_i = \theta_i/(\theta_{i+1} + \varepsilon)$, where ε is a small number to prevent division by zero, and note that in line with what was mentioned above the value of R_i will always fall between zero and one. A value of zero means that tracer is just beginning to penetrate the region; a value of one corresponds to no flux. At each point along the open boundary, after the interior solution has been integrated an increment in time, the following procedure is applied: the value of R_i is computed at the three points prior to the boundary along the normal (let R_0 denote the value of R_i at the boundary): if $R_1 = 0$, then R_0 is set $= 0$; if R_1 is nonzero, then R_0 is predicted using a three-point extrapolation: $R_0 = 3R_1 - 3R_2 + R_3$; if the predicted $R_0 > 1$, R_0 is reset $= 1$; if the predicted $R_0 < 0$, R_0 is reset $= 0$; finally, the concentration of tracer at the boundary is determined from the value of R_0.

For the case of the corner points the extrapolation is performed along the diagonals. This open boundary scheme was tested with purely diffusive examples and led to accurate interior solutions [see Pickart, 1987].

Acknowledgments. The author wishes to acknowledge the help of Nelson Hogg whose ideas helped motivate and shape this work. Bill Young and Dale Haidvogel gave valuable suggestions regarding the set up and analysis of the numerical model. This work was supported by the Office of Naval Research through contracts N00014-76-C-0197 and N00014-84-C-0132, NR 083-400; and N00014-82-C-0019 and N00014-85-C-0001, NR 083-004, and the National Science Foundation through grant OCE82-14925. This is contribution 6517 from the Woods Hole Oceanographic Institution.

REFERENCES

Cessi, P., G. Ierley, and W. Young, A model of the inertial recirculation driven by potential vorticity anomalies, *J. Phys. Oceanogr., 17*, 1640–1652, 1987.

Cox, M. D., An eddy resolving numerical model of the ventilated thermocline, *J. Phys. Oceanogr., 15*, 1312–1324, 1985.

Hogg, N. G., A note on the deep circulation of the western north Atlantic: Its nature and causes, *Deep Sea Res., 30*, 945–961, 1983.

Hogg, N. G., and H. Stommel, On the relationship between the deep circulation and the Gulf Stream, *Deep Sea Res., 32*, 1181–1193, 1985.

Hogg, N. G., R. S. Pickart, R. M. Hendry, and W. J. Smethie, The northern recirculation gyre of the Gulf Stream, *Deep Sea Res., 33*, 1139–1165, 1986.

Holland, W. R., and P. B. Rhines, An example of eddy-induced ocean circulation, *J. Phys. Oceanogr., 10*, 1010–1031, 1980.

McDowell, S., P. Rhines, T. Keffer, North Atlantic potential vorticity and its relation to the general circulation, *J. Phys. Oceanogr., 12*, 1417–1436, 1982.

Musgrave, D. L., A numerical study of the roles of subgyre-scale mixing and the western boundary current on homogenization of a passive tracer, *J. Geophys. Res., 90*, 7037–7043, 1985.

Pickart, R. S., The entrainment and homogenization of tracers within the cyclonic Gulf Stream recirculation gyre, Ph.D. thesis, Mass. Inst. of Technol. and Woods Hole Oceanogr. Inst., Woods Hole, Mass., 1987.

Rhines, P. B., Lectures in geophysical fluid dynamics, in *Fluid Dynam-*

ics in Astrophysics and Geophysics, Lect. Appl. Math., vol. 20, edited by N. R. Lebovitz, pp. 3–5. American Mathematical Society, Providence, R. I., 1983.

Rhines, P. B., and W. R. Young, Homogenization of potential vorticity in planetary gyres, *J. Fluid Mech.*, *122*, 347–367, 1982*a*.

Rhines, P. B., and W. R. Young, A theory of the wind-driven circulation, I, Mid-ocean gyres, *J. Mar. Res., Suppl.*, *40*, 559–596, 1982*b*.

Smith, R. S., Dispersion of tracers in the deep ocean, *J. Fluid Mech.*, *123*, 131–142, 1982.

Smolarkiewicz, P. K., A simple positive definite advection scheme with small implicit diffusion, *Mon. Weather Rev.*, *111*, 479–486, 1983.

R. S. Pickart, Graduate School of Oceanography, University of Rhode Island, Narragansett, RI 02882.

(Received August 10, 1987;
accepted December 11, 1987.)